RSC Advances

RSC Publishing

Corrole-silica hybrid particles: synthesis and effects on singlet oxygen generation†

Joana F. B. Barata, Ana L. Daniel-da-Silva, M. Graça P. M. S. Neves, José A. S. Cavaleiro and Tito Trindade*

The present study describes the first example of hybrid particles composed of amorphous silica and corrole. The hybrid particles were obtained by covalent linking of the gallium(III)(pyridine) complex of 5,10,15 tris(pentafluorophenyl)corrole (GaPFC) at the surface of functionalized silica spheres. The functionalization step was achieved by a nucleophilic substitution reaction between corrole and 3 aminopropyltriethoxysilane previously grafted at the silica surfaces. The hybrids were morphologically and chemically characterized and the results have confirmed covalent linkages between corrole molecules and the silica particles. Preliminary studies on the capacity of corrole and hybrid particles to generate singlet oxygen was evaluated by a chemical method in which 1,3 diphenylisobenzofuran was used to trap singlet oxygen. The new corrole silica hybrid particles have shown lower efficiency to generate singlet oxygen as compared to the pure corrole precursor. This effect was interpreted as a consequence of interparticle interactions mediated by the corrole molecules grafted at the silica surfaces that result in their clustering. Taken together, these findings demonstrate that despite lower efficiency in terms of singlet oxygen generation, the hybrid materials offer an alternative route to develop new platforms with potential for photodynamic therapy.

Introduction

In recent years increased research efforts have been devoted to nanoparticles as novel platforms for therapeutics against cancer cells.[1–4] The association of nanoparticle carriers to photodynamic therapy (PDT) procedures offers great potential to develop new therapeutic systems. PDT involves the use of a photosensitizer (PS) which upon irradiation at a specific wavelength in the presence of oxygen molecules generates cytotoxic singlet oxygen and reactive oxygen species (ROS) which lead to irreversible destruction of cancer cells. Since the efficiency of PDT is dependent on both the irradiation time and dosage of PS, a delivery system that can increase the dosage of PS being delivered into cancer cells is expected to have great advantages in PDT.[5]

The association of PDT drugs to silica surfaces is very promising, namely because silica has been used to coat inorganic nanoparticles and the surfaces can be further functionalized by diverse chemical strategies, thus allowing the development of multifunctional nanomedicines.[6,7] For example, Foscan® encapsulated on silica, has been tested in PDT procedures.[7] Also, porphyrins and phthalocyanines have

already been coupled to a variety of nanoparticles.[8] Porphyrin derivatives have been widely investigated as drugs for cancer treatment essentially due to the high singlet oxygen generation yield and the selectivity to cancer cells.[9] However most porphyrins and related compounds are hydrophobic and have therefore a limited solubility in water.

Corroles form a class of aromatic tetrapyrrolic macrocycles bearing a direct pyrrole–pyrrole linkage. These macrocycles are highly promising molecules in many applications, including the biomedical field.[10] Owing to their unique photochemical properties, corroles are good candidates for PDT applications yet this is an area of medicinal research that has not been explored. In particular, and to the best of our knowledge, there are no reports on the use of corroles that could prompt new advances in PDT photosensitizers based on corrole chemistry. Here we report the first example of a hybrid system in which amorphous silica particles and corrole molecules have been chemically combined.

In order to minimize side reactions, a Ga(III) complex of pentafluorophenylcorrole was selected as a stable corrole derivative in the preparation of the hybrid particles. At this stage, we have favored this aspect in detriment of possible limitations that the use of the Ga(III) corrole complex might have in terms of single oxygen generation as compared to free corrole. Nevertheless, standard assays for singlet oxygen generation of the prepared hybrid Ga(III) corrole complex-silica nanoparticles have been carried out in order to compare

Chemistry Department, CICECO and QOPNA, University of Aveiro, 3810 193, Aveiro, Portugal. E mail: tito@ua.pt; Fax: +351 234 370 084; Tel: +351 234 370 726

their performance for PDT in relation to the use of pure metallocorrole samples.

Experimental

Chemicals

Tetraethylorthosilicate (TEOS) ($Si(OCH_2CH_3)_4$, 98%, Sigma-Aldrich), 3-aminopropyltriethoxysilane (APS) ($H_2N(CH_2)_3Si(OC_2H_5)_3$, 99%, Sigma-Aldrich), ammonia (NH_4OH, 25%, Merck), ethanol (Riedel-de-Haën), 2-propanol (Lab-Scan), acetone (99.9%, AnalR Norma Pur), dimethylformamide (DMF) (($CH_3)_2NCHO$, 99.99%, Fisher Scientific), dichloromethane (CH_2Cl_2, 99.5%, Panreac), 1,3-diphenylisobenzofuran (DPiBF) (95%, Sigma-Aldrich) pentafluorobenzaldehyde (C_6F_5CHO, 95%, Sigma-Aldrich) and gallium(III) chloride ($GaCl_3$, 99%, Sigma-Aldrich) were used as received. Pyrrole (C_4H_4NH, 95%, Sigma-Aldrich) was distilled before use. Toluene (Fluka), dimethyl sulfoxide (DMSO, Fluka) and pyridine (Fluka) were dried using standard procedures. Ultrapure deionized water (resistivity >18 $m\Omega\cdot cm$) was used for preparing aqueous solutions.

Preparation of materials

SYNTHESIS OF CORROLES. The gallium(III)(pyridine)complex of 5,10,15-tris(pentafluorophenyl)corrole (GaPFC) was prepared by complexation of the corresponding free base 5,10,15-tris-(pentafluorophenyl)corrole with $GaCl_3$ in refluxing pyridine according to literature procedures.[11] The free base was synthesized by condensation of pyrrole with pentafluorobenzaldehyde using Gryko's method.[12]

SYNTHESIS OF AMORPHOUS SILICA PARTICLES. Silica particles with an average size of 131.3 $\pm$ 12.7 nm were prepared using the Stöber method[13] by using the hydrolysis of TEOS and subsequent condensation reactions in a homogeneous alcoholic medium in the presence of ammonia. In a typical synthesis a mixture comprising ethanol (41.5 mL), water (4.5 mL), ammonia solution (1.9 mL) and TEOS (2.25 mL) was stirred for 24 h at room temperature.[14] The resulting particles were washed thoroughly with water, collected by centrifugation and dried at room temperature. The surface of silica particles was then modified with the alkoxysilane APS following a procedure described elsewhere.[15]

SYNTHESIS OF CORROLE SILICA HYBRID PARTICLES. GaPFC (9 mg, 9.56 μmol) was added to a suspension of amine surface functionalized silica nanoparticles (98.6 mg) in dry DMSO (1 mL) and the resulting mixture was magnetically stirred during 24 h at 100 °C, under nitrogen atmosphere. The resulting hybrid particles were washed with distilled water, acetone and dichloromethane (in that order). For each solvent the particles were washed four times and centrifuged for 5 min at 14 000 rpm, using a Micro Force 1618 centrifuge. The corrole-silica particles (GaPFC-APS-SiO₂) were dried under vacuum. The corrole content of the resulting hybrid particles was determined by ICP for gallium as 10 wt%.

Photostability of hybrid particles suspensions

The photostability of the GaPFC-APS-SiO₂ particles was evaluated by exposing an aerated suspension of GaPFC-APS-SiO₂ in DMF, to white light (25 W m^{-2}). During irradiation the suspension was magnetically stirred, in a quartz cell, at room temperature. The UV-VIS spectrum of the suspension was recorded at different times of irradiation from 0 to 36 min and the absorbance intensity of the Soret band was monitored and compared with the original one. Similar assays were performed in the dark.

Evaluation of singlet oxygen generation

The ability of the GaPFC-APS-SiO₂ particles to generate singlet oxygen was qualitatively evaluated following the photooxidation of 3-diphenylisobenzofuran (DPiBF) a singlet quencher. The ability of GaPFC was also evaluated for comparison. A stock suspension of GaPFC-APS-SiO₂ particles at 0.01 mM in DMF and stock solutions of GaPFC at 0.5 μM (corresponding to the concentration of corrole complex present in the hybrid) and of DPiBF at 10 mM in DMF were prepared. Reaction mixtures of 50 μM of DPiBF and 0.5 μM of each photosensitizer (PS) in DMF were irradiated, in a glass cell (2 mL), with white light filtered through a cut-off filter for wavelengths <540 nm, at a fluence rate of 25 W m^{-2}.

During the irradiation period, the solutions/suspensions were stirred at room temperature. The percentage of the DPiBF absorption decay, that it is proportional to the production of singlet oxygen, was monitored by measuring the difference between the initial absorbance at 415 nm and the absorbance after a given time of irradiation. The DPiBF absorption decays were measured at irradiation intervals of 1 min up to 15 min.

Instrumentation

The FTIR spectra were collected using a spectrometer Mattson 7000 with 256 scans and 4 cm^{-1} resolution, using a horizontal attenuated total reflectance (ATR) cell. The optical absorption spectra in dry dimethylformamide were recorded in quartz cells using a UV-2501-PC Shimadzu spectrophotometer. The optical absorption spectra in the solid state were recorded using a Jasco V-560 UV-VIS spectrophotometer (Jasco Inc., USA). Fluorescence steady state measurements were carried out with a Fluoromax-3 spectrofluorimeter. Corrected spectra were obtained using the correction file provided with the instrument. All the spectra were recorded at room temperature using a 1 cm path length quartz cuvette. Samples for SEM analysis were prepared by evaporating dilute suspensions of the particles on a copper grid coated with an amorphous carbon film. The samples were analysed using a Hitachi SU-70 scanning electron microscope at an accelerating voltage of 30 kV. Average particle size of corrole-silica hybrids in suspensions was determined by DLS using a Zetasizer Nanoseries instrument from Malvern Instruments. The XPS analysis was performed using a ESCALAB 200A, VG Scientific (UK) with PISCES software for data acquisition and analysis. For analysis, an achromatic Al (K_α) X-ray source operating at 15 kV (300 W) was used, and the spectrometer, calibrated with reference to Ag $3d_{5/2}$ (368.27 eV), was operated in CAE mode with 20 eV pass energy. Data acquisition was performed in
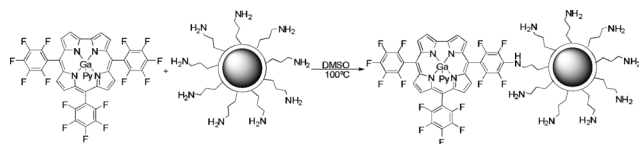
Scheme 1 Synthetic route to silica corrole nanoparticles.

vacuum (P < 10^{-6} Pa). Spectra analysis was performed using peak fitting with Gaussian-Lorentzian peak shape and Shirley type background subtraction (or linear taking in account the data).

Results and discussion

Synthesis and characterization of GaPFC-APS-SiO$_2$ particles

The starting materials include amine functionalized silica particles and Ga(III)(pyridine) complex of 5,10,15-tris(pentafluorophenyl)corrole (GaPFC), a stable pentafluorophenylcorrole complex. These compounds were prepared, according to literature procedures.[11,12] In order to prepare the hybrid particles, an aromatic nucleophilic substitution reaction was carried out between the *para*-fluorine atoms of pentafluorophenyl rings of GaPFC and functionalized silica particles, since the *para*-fluorine atoms of 5 and 15 pentafluoro-phenyl rings are more reactive than that of the 10-substituent.[16] Scheme 1 illustrates the synthetic route to silica-corrole conjugates linked by the most reactive position. Although there is no attempt to detail structural features in this scheme, it should be noted that the pentafluorophenyl rings are not coplanar in relation to the corrole macrocycle.[11]

The grafting reaction was carried out in DMSO at 100 °C. After 24 h, thin layer chromatography (TLC) of the reacting mixture showed that most of the starting GaPFC was converted into a new green-colored material that remained in the

baseline. The resulting solids were filtered and washed with adequate solvents in order to remove the residual unbound corrole.

Fig. 1 shows the ATR-FTIR spectra of corrole and of the SiO$_2$ particles at the distinct surface modification stages. The spectrum of the corrole GaPFC shows the typical vibrational bands expected for this type of macrocycle with the characteristic stretching modes from the pyrrole (ν_{C-H}, ν_{C-C}, and ν_{C-N}) assigned to the absorption bands over the range of 700–1500 cm^{-1},[17] and the bands between 2800 and 3000 cm^{-1} assigned to aromatic C–H stretching. Although less intense, these diagnosis bands appear in the spectra of the GaPFC-APS-SiO$_2$ hybrid particles, with slight shifts, at 752, 963 and 2930 cm^{-1} thus confirming the presence of the corrole in the SiO$_2$ particles. As expected, the spectra of the GaPFC-APS-SiO$_2$ particles is dominated by the typical bands of amorphous SiO$_2$ at 1035 cm^{-1} (ν_{as}(SiO–Si)), 947 cm^{-1} (ν(Si–OH)) and 790, 560 and 430 cm^{-1} (δ(Si–O–Si)).[15] The ATR-FTIR spectra of the materials were recorded after washing thoroughly, which in principle removed GaPFC not chemically bound to the silica surface. Moreover, the band corresponding to the CH$_2$ rocking from the Si–CH$_2$R moieties at the silica surface is noticeable at 690 cm^{-1}, which seems to support the presence of covalent linkages between the corrole and the silicon alkoxide linker grafted at the silica surface.[18] These results were further supported by XPS as will be discussed below.

In order to confirm that the corrole macrocycle is covalently linked to the APS functionalized SiO$_2$ particles, a mixture of non-functionalized silica and the complex GaPFC was submitted to heat treatment using the same experimental conditions described for the GaPFC-APS-SiO$_2$ particles synthesis – DMSO at 100 °C. The resulting powder collected after washing was colorless as observed for non-functionalized silica samples. Conversely, the powders resulting from the reaction of GaPFC with the amine functionalized NPs showed a green color, as described above. Accordingly, the UV-VIS spectrum of the GaPFC-APS-SiO$_2$ sample (Fig. 2) shows the GaPFC characteristic Soret band at 450 nm, which is red shifted in relation to that of the pure complex (434 nm). The explanation for this band shift will be apparent later, but for the moment these experiments provided additional evidence for the covalent attachment of GaPFC at the SiO$_2$ surfaces *via* APS linkers. The broadening of the Q band in the spectrum of the SiO$_2$-grafted-corrole can be
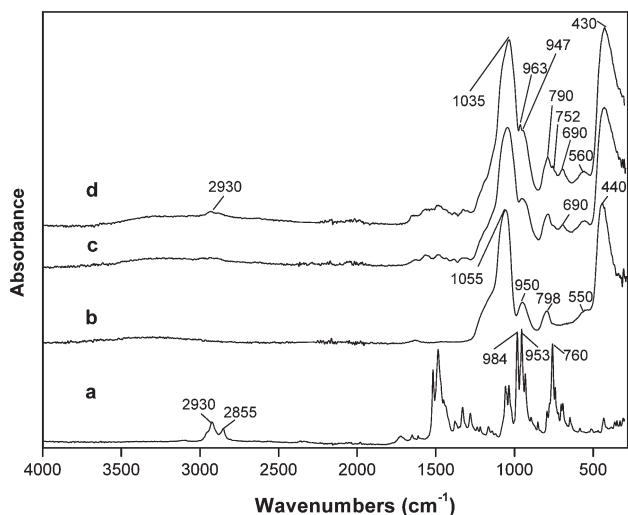
Fig. 1 ATR FTIR spectra: (a) GaPFC, (b) SiO$_2$, (c) SiO$_2$ APS and (d) GaPFC APS SiO$_2$ NPs.
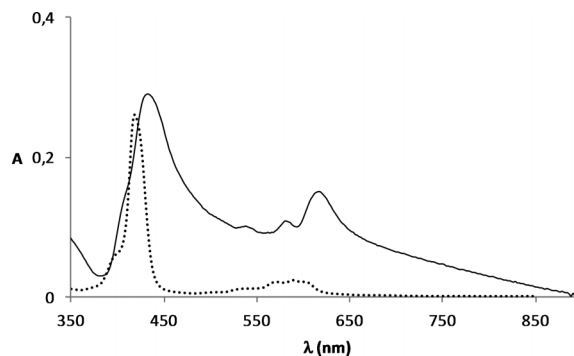
Fig. 2 Absorption spectra of GaPFC (....) and GaPFC APS silica (   ) in ethanol.

Table 1 Binding energies of C 1s, N 1s, F 1s and Ga 2p$_{3/2}$ and bond assignments determined by XPS

Sample	C 1s (eV)	N 1s (eV)	F 1s (eV)	Ga 2p$_{3/2}$ (eV)
GaPFC	285.0 C C	398.3 (iminic type)	688.5 C F	1118.1
	286.2 C H			
	288.3 C N aromatic	400.5 (aminic type)	690.7 C F	
	290.3 C F			
APS SiO$_2$	280.4 Si C	399.7 N H		
	281.8 C C			
	285.2 C N			
GaPFC APS SiO$_2$	284.9	398.1	687.4	1117.5
	285.2	399.1	689.0	
	286.1	399.6	690.4	
	286.9	401.1		

related to aggregation effects of the functionalized particles, due to their low solubility in ethanol.

In order to have a better description of the chemical composition of the hybrid, XPS analysis was performed for samples GaPFC-APS-SiO$_2$, SiO$_2$-APS and GaPFC. The binding energies of C 1s, N 1s, F 1s and Ga 2p$_{3/2}$ are summarized in Table 1.
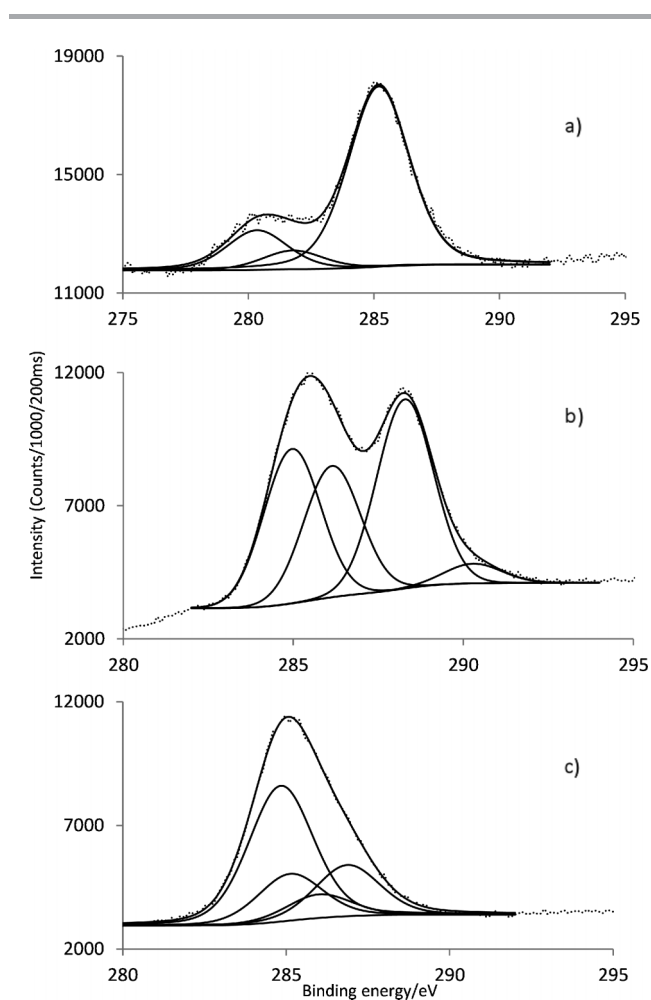

Fig. 3 Characteristic C 1s core line signal of (a) APS SiO$_2$, (b) GaPFC and (c) GaPFC APS SiO$_2$.

The high resolution C 1s signal for SiO$_2$-APS (Fig. 3a) was fitted into three components at 280.4 (SiCH$_2$C), 281.8 (CCH$_2$C) and 285.2 (CH$_2$NH$_2$) eV (Table 1), attributed to the three different carbon atoms in the APS molecule.

For GaPFC (Fig. 3b) the C 1s peak shows four components centered at 285.0, 286.2, 288.3 and 290.3 eV due to the different sorts of C linkages: C–C, C–H, C–N and C–F. The signal at 290.3 eV corresponds to the C–F linkage of the pentafluorophenyl rings.[19] Considering the high resolution C 1s of GaPFC-APS-SiO$_2$ (Fig. 3c) the C linkages of APS and GAPFC contribute to the C 1s signal. Note that the C 1s peak corresponding to the C–N covalent bond between the corrole macrocycle and the silica nanoparticle is observed at 286.9 eV.[20] In fact, all the C 1s peaks of GaPFC-APS-SiO$_2$ have been shifted towards lower energy in relation to free GaPFC, which confirms that a new chemical environment has been established. These observations are consistent with electron-donating effects *via* the APS-SiO$_2$ component.[21,22]

Concerning the high resolution of N 1s (Fig. SI3†), the signal was fitted into one component at 399.7 eV for SiO$_2$-APS (free amine group from APS), two components centered at 400.5 eV (pyrrolic aminic type) and 398.3 eV (pyrrolic iminic type) for GaPFC.[23,24]

The high resolution N 1s signal of GaPFC-APS-SiO$_2$ (Fig. SI 3c†) was fitted into four components centered at 398.1, 399.1, 399.6 and 401.1 eV. These components are due to the four different types of N for the respective chemical linkages present, *i.e.* the free amino group from APS, the *aminic* and *iminic* nitrogens of the corrole core and the new covalent linkage formed between corrole and the silica particles (–C–N–C).[25]

Fig. 4a and b shows the high resolution of F 1s signal for GaPFC and GaPFC-APS-SiO$_2$, respectively. For GaPFC (Fig. 4a) the F 1s peak was fitted to two components centered at 688.5 and 690.7 eV.[26] This assignment takes into account that the 10 pentafluorophenyl ring is distinct from the 5 and 15 rings based on symmetry arguments. The 5 and 15 pentafluorophenyl rings are equivalent in relation to the symmetry plane perpendicular to the corrole macrocycle and that contains the remaining 10 pentafluorophenyl ring, which is distinct.[11] The shape of the F 1s signal peak (Fig. 4b) for the GaPFC-APS-SiO$_2$ is similar to GaPFC, however with a more intense shoulder at 690.4 eV probably due to chemical modification on the periphery of the pentafluorophenyl rings, with the new formed
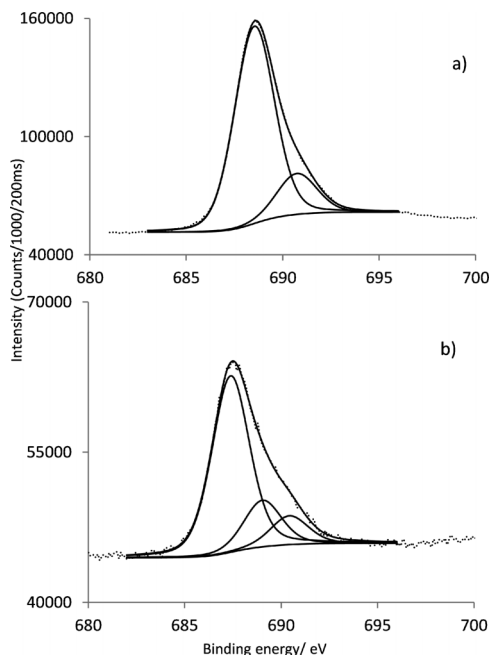
Fig. 4 Characteristic F 1s core line signal of (a) GaPFC and (b) GaPFC APS SiO$_2$.

Fig. 6 Reduction of DPiBF absorbance in the presence of GaPFC and of GaPFC APS SiO$_2$ NPs at different concentrations after 15 min of irradiation with white light filtered through a cut off filter for wavelengths <540 nm (25 W m^{-2}). Concentrations indicated for the GaPFC APS SiO$_2$ refer to the equivalent concentration of non immobilized GaPFC.

linkages to the APS-SiO$_2$ particles. Note that Scheme 1 shows an oversimplified view of the derivatized amorphous SiO$_2$ particles because it does not show surface sites with distinct environments. Concerning the high resolution of Ga 2p$_{3/2}$ for the GaPFC-APS-SiO$_2$ its binding energy and shape is similar to the ones of corrole complex GaPFC (Table 1, Fig. SI4†).

Photostability and singlet oxygen generation

As a first step to assess the potential of the GaPFC-APS-SiO$_2$ hybrids as photosensitizers in PDT, the respective photo-stability under light irradiation was evaluated and compared to that of the pure complex. This aspect is crucial because similarly to porphyrin derivatives, corroles can go through photobleaching when exposed to UV-VIS light and oxygen. A fast photobleaching would cause the concentration of the drug to decrease, thus impairing its effectiveness as a photosensi-
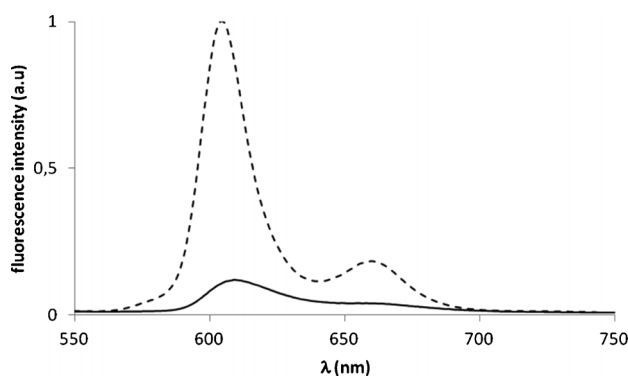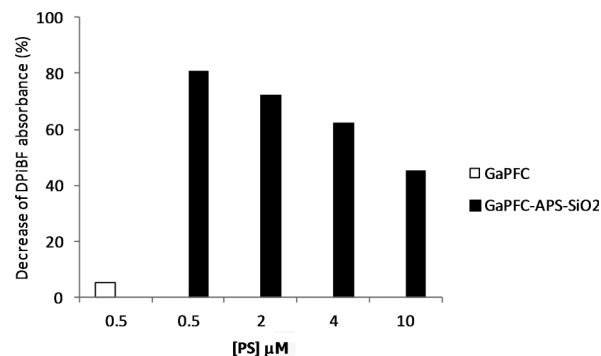
tizer in PDT.[27] The UV-VIS spectra of GaPFC-APS-SiO$_2$ suspensions during the total irradiation period (see Fig. SI1 in the ESI†) did not show significant absorbance decay of the Soret and Q bands when compared to similar assays performed in dark conditions, thus pointing out that GaPFC-APS-SiO$_2$ particles are photostable under light irradiation conditions.[28]

Also, the fluorescence emission spectra of GaPFC and GaPFC-APS-SiO$_2$ particles show maxima at 605 nm and 660 nm, thus indicating that the corrole units in the silica act as emitting centers (Fig. 5).[29]

To evaluate the potential of GaPFC-APS-SiO$_2$ hybrids as photosensitizers for PDT, its capacity to generate singlet oxygen was estimated using 1,3-diphenylisobenzofuran (DPiBF) as a ^{1}O$_2$ indicator. This is a standard indirect test in which yellow DPiBF is oxidized with ^{1}O$_2$ via a Diels–Alder cycloaddition reaction to colorless o-dibenzoylbenzene. There were no attempts here to detail the photophysics of these systems, but instead to provide a preliminary assessment of the effect of the silica nanoparticles on the corrole capacity to generate ^{1}O$_2$. As such, the DPiBF absorption band at 415 nm was monitored to follow the ability of the PS to generate ^{1}O$_2$.[23] Fig. 6 summarizes data for the absorption decay observed at 415 nm for the analysed samples. It is clear from these results that GaPFC-APS-SiO$_2$ hybrids are able to generate ^{1}O$_2$ that
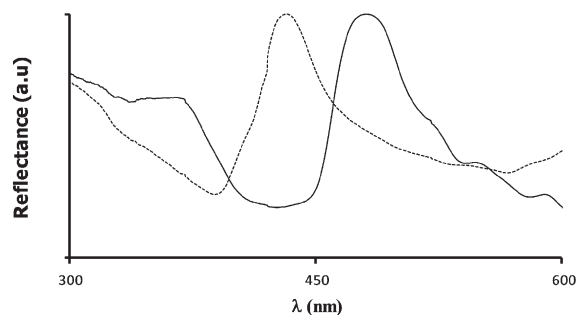

Fig. 5 Fluorescence emission spectra of GaPFC (   ) and of GaPFC APS SiO$_2$ particles (   ) in DMF. Excitation wavelength at 417 nm, OD 0.08.

Fig. 7 Visible reflectance spectra of GaPFC (   ) and GaPFC APS SiO$_2$ (   ).

depends on the concentration employed but are also less efficient as compared to non-immobilized GaPFC complex.

In a first attempt to explain the lower efficiency of the hybrids for $^1O_2$ generation as compared to pure GaPFC, the role of the SiO_2 particles was investigated by a control experiment in which a blend of the components was used.[30] Thus GaPFC was mixed either with non-functionalized (SiO_2) or functionalized (APS-SiO_2) silica particles and the respective DPiBF absorption decays have been evaluated (Fig. SI6†). The results obtained in both cases after 15 min of light irradiation were similar.

A possible explanation relies on the distinct optical properties observed for the GaPFC and derived silica hybrids (Fig. 2 and 5). First we note that the UV-VIS spectrum of GaPFC-APS-SiO_2 shows a slight batochromic shift (16 nm) of the Soret band in relation to the spectrum of the pure complex in solution (Fig. 2). This might be an indication that the GaPFC molecules grafted at the silica surfaces are interacting due to their proximity as a result of particle aggregation. This tendency would be expected to be more pronounced in the solid state and in fact, the visible reflectance spectrum of the corresponding GaPFC-APS-SiO_2 powder (Fig. 7) shows a larger batochromic shift (37 nm).

The morphological characteristics of the starting SiO_2 particles and of the GaPFC-APS-SiO_2 sample were analyzed by scanning electron microscopy (SEM). As expected from previous reports, the as prepared SiO_2 particles appear as discrete particles dispersed on the sample[14] (Fig. 8a). Also DLS measurements performed on APS functionalized colloids gave an average particle diameter of 158 nm. Therefore, prior functionalization with the corrole derivative, the SiO_2 colloid is mainly composed of discrete particles as the dispersible phase. On the other hand, GaPFC-APS-SiO_2 particles deposited from suspensions of a variety of organic solvents, such as acetone, ethanol and DMF, originated blackberry-shaped clusters composed of spherical SiO_2 particles (Fig. 8). Additionally, clustering was still observed for samples deposited from aqueous suspensions at pH 4 and pH 9 in variable

extent (Fig. SI5†). Dynamic Light Scattering (DLS) experiments performed on these suspensions suggest that this clustering effect had already occurred in solution and is not a result from SEM specimen preparation. In fact, the average diameter (and standard deviation) determined by DLS for the GaPFC-APS-SiO_2 dispersed in water was 229.7 ± 3.5 nm and the suspensions at pH 4 and pH 9 result in particle average sizes of 497.0 ± 17.6 nm and 576.7 ± 29.7 nm, respectively. Therefore, these results indicate that this clustering effect is a consequence of the GaPFC attached at the silica particle surfaces and depends on the dispersing medium. In fact, for GaPFC-APS-SiO_2 particles dispersed in DMF, i.e. the solvent used for $^1O_2$ measurements, an average diameter of 463.0 ± 33 nm was obtained which is consistent with the dimensions observed for the particle clusters in the SEM images (Fig. 8).

The above discussion is consistent with a self-assembly process in which the clustering of the hybrid particles is mediated by the interactions occurring between adjacent corrole macrocycles. In fact, the establishment of π–π interactions between the corrole molecules at the SiO_2 surface would account for the optical features shown in Fig. 7.[31–33] Also, the role of the corrole complex as a molecular spacer for directional assembly can not be discarded, because each corrole complex has three available sites to react with each amine group at the SiO_2 surface. However this effect has to be balanced with particle size constraints arising from the proximity of neighboring SiO_2 particles.

Conclusions

We have successfully prepared corrole-silica hybrid particles using a methodology that led to covalent bonding of a corrole photosensitizer to amorphous SiO_2 previously modified with APS. The GaPFC-APS-SiO_2 hybrid particles show less capability to generate $^1O_2$ when compared to the non-immobilized complex. A process of particles clustering mediated by the GaPFC molecules was proposed as an explanatory hypothesis for this effect, on the basis of evidence gathered by electron microscopy and optical measurements. On the other hand, because silica is a versatile chemical platform for chemical derivatization, this research opens a new avenue to produce multifunctional particles for PDT using corroles as photosensitizers. In this way, the lower efficiency observed for the hybrid particles can be balanced by other possibilities of using this type of surface chemistry in new PDT platforms.
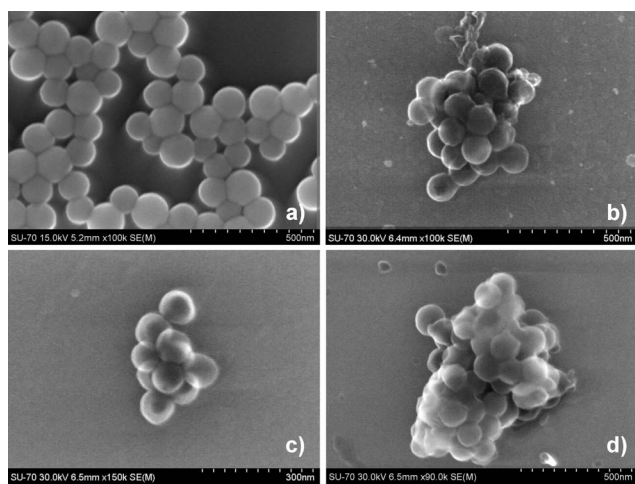

Fig. 8 SEM images a) SiO_2, b) GaPFC APS SiO_2 deposited from acetone, c) GaPFC APS SiO_2 deposited from ethanol and d) GaPFC APS SiO_2 from DMF.

Acknowledgements

References

1 D. Bechet, P. Couleaud, C. Frochot, M.-L. Viriot, F. Guillemin and M. Barberi-Heyob, *Trends Biotechnol.*, 2008, **26**, 612.

2 D. K. Chatterjee, L. S. Fong, Y. Zhang, D. K. Chatterjee, L. S. Fong and Y. Zhang, *Adv. Drug Delivery Rev.*, 2008, **60**, 1627.

3 Y. Cheng, J. D. Meyers, A.-M. Broome, M. E. Kenney, J. P. Basilion and C. Burda, *J. Am. Chem. Soc.*, 2011, **133**, 2583.

4 T. D. Schladt, K. Schneider, M. I. Shukoor, F. Natalio, H. Bauer, M. N. Tahir, S. Weber, L. M. Schreiber, H. C. Schröder, W. E. G. Müllerb and W. Tremel, *J. Mater. Chem.*, 2010, **20**, 8297.

5 J. Zhu, H. Wang, L. Liao, L. Zhao, L. Zhou, M. Yu, Y. Wang, B. Liu and C. Yu, *Chem.–Asian J.*, 2011, **6**, 2332.

6 L. M. Rossi, P. R. Silva, L. L. R. Vono, A. U. Fernandes, D. B. Tada and M. S. Baptista, *Langmuir*, 2008, **24**, 12534.

7 P. Couleaud, V. Morosini, C. Frochot, S. Richeter, L. Raehm and J.-O. Durand, *Nanoscale*, 2010, **2**, 1083.

8 B. Roszek, W. H. Jong and R. E. Geertsma, *Nanotechnology in medical applications: state-of-the-art in materials and devices*, RIVM report 265001001/2005.

9 R. Bonnett, *Chemical Aspects of Photodynamic Therapy*, Gordon and Breach Science Publishers, London, 2000.

10 I. Aviv and Z. Gross, *Chem. Commun.*, 2007, 1987.

11 J. Bendix, I. J. Dmochowski, H. B. Gray, A. Mahammed, L. Simkhovich and Z. Gross, *Angew. Chem., Int. Ed.*, 2000, **39**, 4048.

12 D. T.; Gryko and B. Koszarna, *Org. Biomol. Chem.*, 2003, **1**, 350.

13 W. Stöber, A. Fink and E. Bohn, *J. Colloid Interface Sci.*, 1968, **26**, 62.

14 R. J. B. Pinto, P. A. A. P. Marques, A. M. Barros-Timmons, T. Trindade and C. P. Neto, *Compos. Sci. Technol.*, 2008, **68**, 1088.

15 P. I. Girginova, A. L. Daniel-da-Silva, C. B. Lopes, P. Figueira, M. Otero, V. S. Amaral, E. Pereira and T. Trindade, *J. Colloid Interface Sci.*, 2010, **345**, 234.

16 T. Hori and A. Osuka, *Eur. J. Org. Chem.*, 2010, 2379.

17 J. Rochford, D. Chu, A. Hagfeldt and E. Galoppini, *J. Am. Chem. Soc.*, 2007, **129**, 4655.

18 B. Lee, Y. Kim, H. Lee and J. Yi, *Microporous Mesoporous Mater.*, 2001, **50**, 77.

19 P. G. Gassman, A. Ghosh and J. Almlof, *J. Am. Chem. Soc.*, 1992, **114**, 9990.

20 J. F. Moulder, W. F. Stickle, P. E. Sobol and K. D. Bomben, *Handbook of X-ray Photoelectron Spectroscopy, A Reference Book of Standard Spectra for Identification and Interpretation of XPS Data*, Physical Electronics, Inc., 1995.

21 L. Bekalé, S. Barazzouk and S. Hotchandani, *J. Mater. Chem.*, 2012, **22**, 2943.

22 D. M. Sarno, L. J. Matienzo and W. E. Jones, *Inorg. Chem.*, 2001, **40**, 6308.

23 J. M. Gottfried, K. Flechtner, A. Kretschmann, T. Lukasczyk and H.-P. Steinrück, *J. Am. Chem. Soc.*, 2006, **128**, 5644.

24 D. Karweik and H. Winograd, *Inorg. Chem.*, 1976, **15**, 2336.

25 C. Perruchot, M. M. Chehimi, D. Mordenti, M. Briand and M. Delamar, *J. Mater. Chem.*, 1998, **8**, 2185.

26 X. Miao, A. Gao, S. Hiroto, H. Shinokubo, A. Osuka, H. Xin and W. Deng, *Surf. Interface Anal.*, 2009, **41**, 225.

27 V. V. Serra, A. Zamarrón, M. A. F. Faustino, M. C. I. Cruz, A. Blázquez, J. M. M. Rodrigues, M. G. P. M. S. Neves, J. A. S. Cavaleiro, A. Juarranz and F. Sanz-Rodríguez, *Bioorg. Med. Chem.*, 2010, **18**, 6170.

28 C. M. B. Carvalho, E. Alves, L. Costa, J. P. C. Tomé, M. A. F Faustino, M. G. P. M. S. Neves, A. C. Tomé, J. A. S. Cavaleiro, A. Almeida, Â. Cunha, Z. Lin and J. Rocha, *ACS Nano*, 2010, **4**, 7133.

29 S. Tao and G. Li, *Colloid Polym. Sci.*, 2007, **285**, 721.

30 M. Pineiro, S. M. Ribeiro and A. C. Serra, *Arkivoc*, 2010, **5**, 51.

31 S. Tanaka, M. Shirakawa, K. Kaneko, M. Takeuchi and S. Shinkai, *Langmuir*, 2005, **21**, 2163.

32 R. van Hameren, J. A. A. W. Elemans, D. Wyrostek, M. Tasior, D. T. Gryko, A. E. Rowan and R. J. M. Nolte, *J. Mater. Chem.*, 2009, **19**, 66.

33 V. V. Serra, S. M. Andrade, M. G. P. M. S. Neves, J. A. S. Cavaleiro and S. M. B. Costa, *New J. Chem.*, 2010, **34**, 2757.